Quantum Cascade Lasers

W. Schrenk, S. Anders, C. Pflügl, E. Gornik, G. Strasser

Institute for Solid State Electronics, Vienna University of Technology

In this work, we intend to present our latest results on the improvement of GaAs/AlGaAs QCLs. The emission wavelength of the mid infrared lasers covers now a range from 8.7 µm up to 23 µm. Room temperature operation is now achieved for several band structure designs.

Introduction

Quantum cascade lasers (QCLs) are powerful light emitters in the mid infrared and, most recently, also in the far infrared [1]. The light generation is based on intersubband transitions, usually within the conduction band. The strong light emission in the mid infrared spectral region is interesting for chemical sensing, and a potential application for far infrared emission is astronomy and tomography in medicine. Recently, continuous wave operation at room temperature of InP based QCLs has been demonstrated [2].

Theory

The design of the band structure of quantum cascade lasers is a challenging task. The population of the individual levels is determined by different scattering processes like electron-electron scattering, LO-phonon emission or absorption, and photon emission or absorption. The population of the energy levels together with the position of the doping atoms modifies the band edge energy. Almost all laser structures are designed so far by very simple one-band calculations, based on an effective mass approximation. The band structures are calculated neglecting the electron population and assuming a constant electric field across each cascade. The non-parabolicity of the energy dispersion is taken into account by an energy dependent effective mass [3]. Only for a few designs more sophisticated calculations were done afterwards, because they are too time consuming to be used as design tool [4], [5].

The advantage of AlGaAs/GaAs grown on GaAs over InGaAs/InAlAs grown on InP is that the $Al_xGa_{1-x}As$/GaAs material system is lattice matched to GaAs for all Al contents x. The Al-content of QCLs working at room temperature in pulsed operation is x=0.45. The emission wavelength of these lasers is in the range of 9 µm [6], [7] up to 12.6 µm [8]. The barrier height in respect to the GaAs wells is 390 meV, large enough to prevent carrier escape into the continuum. In the case of a longer emission wavelength, a lower Al-content is preferred in order to obtain a reasonable thickness of at least one monolayer for the thinnest barrier. Another advantage of GaAs is the far infrared performance. Undoped InP substrates have a rather high background doping which causes free carrier absorption.

The band structure of a chirped superlattice design is shown in Fig. 1 [8]. The laser transition takes place between the lowest level of the second miniband and the highest level of the first miniband. The optical matrix element is large but the total lifetime in the upper laser level is short as LO phonon emission is possible to many final states in the first miniband. In the case of a three well design [6], fewer levels are below the upper laser level, and therefore the total lifetime in the upper laser level is longer. A drawback

of the three well design is the lower optical dipole matrix element in comparison to a chirped superlattice design and the slower carrier extraction form the lower laser level.

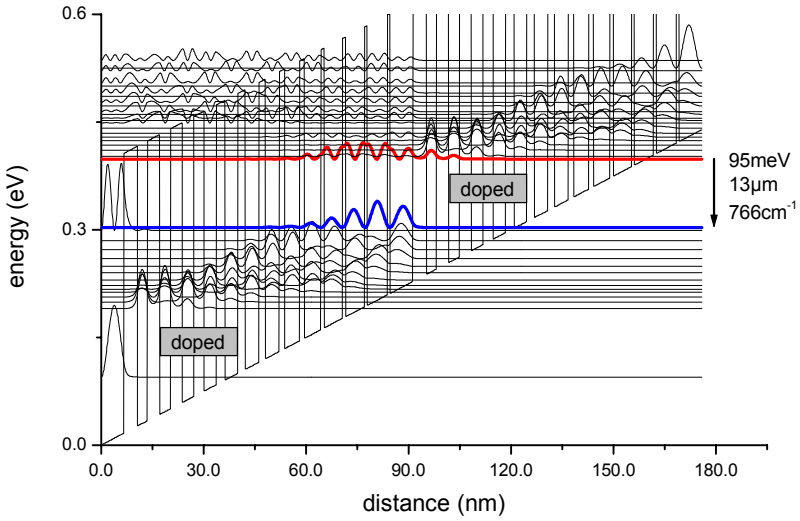

Fig. 1: Calculated conduction band diagram and squared wave functions of a chirped superlattice design for emission at 13 µm wavelength.

Experimental

Sample Preparation

The laser material is grown by molecular beam epitxy on (100) GaAs substrates. The gain media is embedded in the most cases in a double plasmon enhanced waveguide. Such a waveguide consists of ~1 µm thick highly doped cladding layers (~4x10^{18} cm^{-3}), and ~3.5 µm thick low doped spacer layers (~4x10^{16} cm^{-3}). The highly doped layers are used for light confinement and the spacer layers reduce the penetration of the guided mode into the cladding layers as they show huge free carrier absorption. A surface plasmon waveguide [9] is usually used for long wavelength material (λ > 20 µm) because of the reduced thickness, which is important for MBE growth.

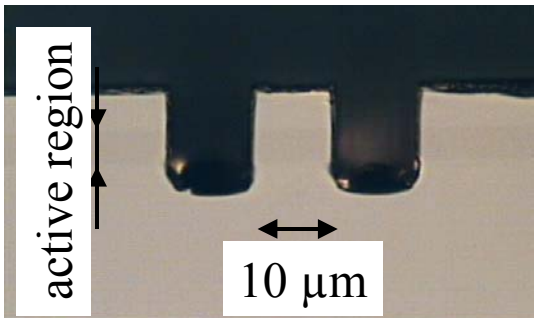

Fig. 2: Image of a laser facet of a 10 µm wide FP laser. The trenches are etched by reactive ion etching.

Different cavity types such as Fabry Perot (FP), distributed feedback (DFB), and cylinder lasers were fabricated. Reactive ion etching was used for directional etching to obtain vertical etch profiles (Fig. 2). SiN is used for insulation and the extended contacts are sputtered. The grating for the DFB lasers was etched into the surface of the top cladding layer and covered with metal. The light is confined by total internal reflection in the case of cylinder shaped lasers. The lasers were soldered with In on Cu plates and wire bonded.

Measurements

Spectral measurements were performed with a Fourier Transform Infrared (FTIR) spectrometer. The absolute light power was measured with a thermopile detector, and the optical power versus current curves were measured in some cases with a DTGS detector or LN_2 cooled MCT detectors, depending on the optical power. Typical operation conditions are 100 ns long pulses and repetition rates in the order of 5 kHz up to several MHz. Pulsed room temperature operation (Fig. 3) was achieved for three different design strategies, a three well design [6], a chirped superlattice design [8], and a bound to continuum design. A bound to continuum design combines the advantages of the three well design and the chirped superlattice and allowed pulsed operation up to 100°C.

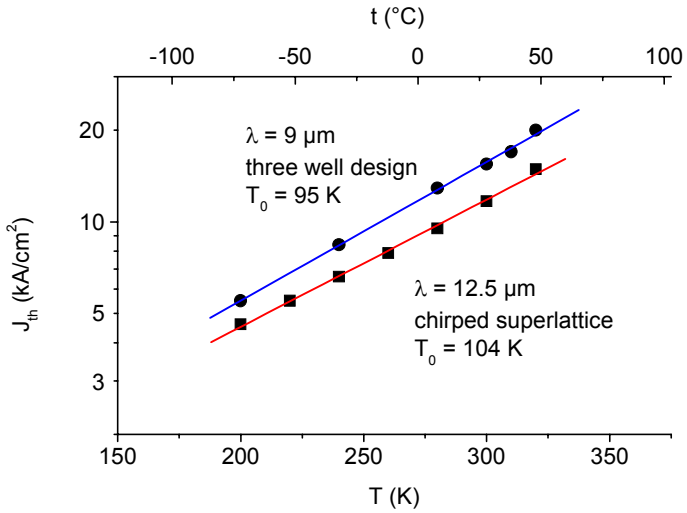

Fig. 3: Threshold current density of cylinder lasers as a function of the heat sink temperature for a three well design (circles) and a chirped superlattice (squares). The lines are fits of the characteristic temperature T_0 ($J_{th} = J_0 \exp(T/T_0)$).

Acknowledgements

This work was supported by the European Community-IST Project SUPERSMILE, and the Austrian FWF (ADLIS).

References

[1] R. Köhler, A. Tredicucci, F. Beltram, H. E. Beere, E. H. Linfield, A. G. Davies, D. A. Ritchie, R. Iotti, F. Rossi: “Terahertz heterostructure laser”, Nature, vol. 417, 2002, pp. 156–159.

[2] M. Beck, D. Hofstetter, T. Aellen, J. Faist, U. Oesterle, M. Ilegems, E. Gini, H. Melchior: “Continuous Wave Operation of a Mid-Infrared Semiconductor Laser at Room Temperture”, Science, vol. 295, 2002, pp. 301–305.

[3] C. Sirtori, F. Capasso, J. Faist, S. Scandolo: “Nonparabolicity and sum rule associated with bound-to-bound and bound-to-continuum intersubband transitions in quantum wells”, Phys. Rev. B, vol. 50, 1994, pp. 8663–8674.

[4] R. Iotti, F. Rossi: “Nature of Charge Transport in Quantum-Cascade Lasers”, Phys. Rev. Lett., vol. 87, 2001, pp. 146603-1–146603-4

[5] A. Wacker, S. C. Lee: “Gain and loss in quantum cascade lasers”, Physica B, vol. 314 (1-4), 2002, pp. 327–331.

[6] H. Page, H. Page, C. Becker, A. Robertson, G. Glastre, V. Ortiz, C. Sirtori: “300 K operation of a GaAs-based quantum-cascade laser at □≈9 μm”, Appl. Phys. Lett., vol. 78, 2001, pp. 3529–3531.

[7] W. Schrenk, E. Gornik, H. Page, C. Sirtori, V. Ortiz, G. Strasseri: “High performance single mode GaAs quantum cascade lasers”, Physica E, vol. 13, 2002, pp. 840–843.

[8] S. Anders, W. Schrenk, E. Gornik, G. Strasser: “Room-temperature emission of GaAs/AlGaAs superlattice quantum-cascade lasers at 12.6 μm”, Appl. Phys. Lett., vol. 80, 2002, pp. 1864–1866.

[9] J. Ulrich, J. Kreuter, W. Schrenk, G. Strasser, K. Unterrainer: “Long wavelength (15 and 23 μm) GaAs/AlGaAs quantum cascade lasers”, *Appl. Phys. Lett.,* vol. 80, 2002, pp. 3691–3693.